J Intell Robot Syst (2012) 65:175–186
DOI 10.1007/s10846-011-9575-3

Mini Rotorcraft Flight Formation Control Using Bounded Inputs

Jose Alfredo Guerrero · Pedro Castillo · Sergio Salazar · Rogelio Lozano

Received: 15 February 2011 / Accepted: 18 April 2011 / Published online: 17 August 2011

Abstract In this paper, the flight formation control and trajectory tracking control design of multiple mini rotorcraft systems are discussed. The dynamic model of a mini rotorcraft is presented using the Newton-Euler formalism. Our approach is based on a leader/follower structure of multiple robot systems. The centroid of the coordinated control subsystem is used for trajectory tracking purposes. A nonlinear controller based on separated saturations and a multi-agent consensus algorithm is developed. The analytic results are supported by simulation tests. Experimental results include yaw coordination and tracking only.

This material is based on work supported by the project SIRENE CARNOT CA10/154 UTC.

J. A. Guerrero (✉) · P. Castillo · R. Lozano
Université de Technologie de Compiègne, Heudiasyc UMR CNRS 6599, Compiègne, France
e-mail: jguerrer@hds.utc.fr

P. Castillo
e-mail: castillo@hds.utc.fr

R. Lozano
e-mail: rlozano@hds.utc.fr

S. Salazar
LAFMIA-UMI CNRS 3175, Mexico City, Mexico

Keywords Flight formation · Coordination control · Quadrotor

1 Introduction

Unmanned Aerial Vehicles (UAVs) have become a vital platform in a wide variety of applications because they reduce cost and human life risk. Multiple aircraft flying in formation has been intensively investigated during the last decades [1–5]. Different approaches for multiple aircraft flying in formation have been proposed in the literature for coordination of multiple autonomous robot systems such as Leader/Follower [1–3] Virtual Structure [4, 5] and Behavioral Control [6, 7].

The miniature rotorcraft flight formation control involves the integration of different domains such as, rotorcraft control, coordination control among others. The work reported in the literature is by now quite vast and addresses different approaches for miniature rotorcraft stabilization including linear control [8–10], robust control [9, 11, 12], nonlinear control [2, 13, 14] among others. In [9], the authors propose a robust linear PD controller considering parametric interval uncertainty. There, the authors present a robust stability analysis and compute the robustness margin of the system with respect to the parameters uncertainty. In [14] a nonlinear control based on nested

saturations is presented. In this approach, the dynamics is decoupled into lateral and longitudinal dynamical subsystems. Thus, nested saturations control was used to stabilize each subsystem.

In the last decade, graph theory has been used in order to model the communication between agents in a multi-agent system. In a graph theoretical approach to flight formation, every node in the graph is considered as an agent or aerial vehicle which can have information exchange with all or several agents. In [5, 15–17], the authors use algebraic graph theory in order to model the information exchange between vehicles. By using this technique, several control strategies have been developed, e.g. [17–21]. In [17], the authors present several algorithms for consensus and obstacle avoidance for multiple-agent systems. Ren [18] presents a consensus algorithm for trajectory tracking of a time varying reference for a single integrator multi-agent system. Lee and Li [19] and Lee and Spong [20] presents a passive decomposition approach for consensus and formation control. In [21], the authors present a bilateral teleoperation control approach for the multi-agent coordination and trajectory tracking problem.

Recent advances in UAV control, graph theory and the technological revolution of the last decades have spurred the interest in the UAV flight formation problem. In [2] a flight formation control based on a forced consensus algorithm is presented. Experimental results on cooperative and coordination control of UAVs have been obtained using the Vicon motion capture system, see [22, 23] among others. Michael et al. [22] presents a cooperative control strategy to lift a rigid body using three quadrotors. From the practical point of view, we remark that the Vicon system is an indoor localization system which parameterize the 3D space using a set of infrared cameras. The main advantage of this system is the accuracy (millimeters) and the processing speed (100–400 Hz). However, the main disadvantages of this system are its price which is expensive and the fact that it cannot be used in real outdoor missions. Another important disadvantage of the Vicon system is the centralized nature of the localization system.

We are interested in the problem of multiple miniature rotorcraft flying in formation, shown in Fig. 1, using a nonlinear control based on separated saturations and a single integrator coordination control strategy. The coordination algorithm assumes that there are n-aerial vehicles which have some kind of information exchange between them. In this approach, every mini rotorcraft is considered as an agent in the multi-agent system. We propose a decoupled dynamic coordination. Thus, the lateral, longitudinal, heading and altitude dynamical subsystems of each mini rotorcraft are considered as agents to be coordinated and to follow a desired reference. To do this, combined with a nonlinear control, we use an algebraic graph theoretical approach to synchronize the behavior of a miniature rotorcraft platoon.

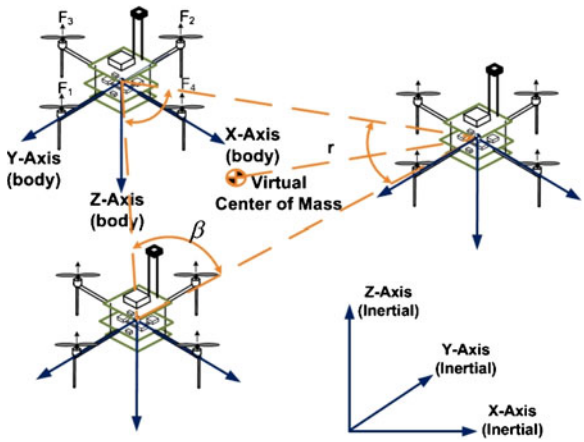

Fig. 1 Multiple mini rotorcraft flying in formation [2]

In order to achieve consensus among the members of the platoon, we propose a single integrator coordination which implies position coordination only. An important advantage of the approach adopted here is that a member of the platoon will not be affected by perturbations in the attitude of its neighbors. Experimental results have been implemented using two experimental prototypes provided of a wireless communication system. Position experimental results are still under development due to the lack of accuracy of the commercial mini-GPS (Global Positioning System) modules (small-size, small weight) available in the market.

This paper is organized as follows: in Section 2 some preliminary results on graph theory, saturation function and the dynamical model of a

minirotorcraft are given. In Section 3, the nonlinear control algorithm is obtained. Simulation and experimental results are discussed in Section 4. Finally, the conclusions and future work are presented in Section 5.

2 Preliminaries

2.1 Graph Theory

A multi-agent dynamic system can be modelled as a group of dynamical systems which has an information flow or information exchange topology represented by information graphs. A graph $\mathcal{G}$ is a pair $\mathcal{G}(\mathcal{N}, \mathcal{E})$ consisting of a set of nodes $\mathcal{N} = \{n_i : n_i \in \mathcal{N}, \forall i = 1, ..., n\}$ together with their interconnections $\mathcal{E}$ on $\mathcal{N}$ [24]. Each pair (n_1, n_2) is called an edge $e \in \mathcal{E}$. An undirected graph is one where nodes i and j can get information from each other. In a digraph, the ith node can get information from the jth node but not necessarily vice versa. We can think of the information exchange between agents as an undirected graph but also as a digraph which implies a more complicated problem. One important characterization of graphs is their connectivity. A graph is said to be connected if for every pair (n_1, n_2) of distinct nodes there is a path from n_1 to n_2. A connected graph allows the communication between all agents through the network. A directed graph is said to be strongly connected if any two nodes can be joined by a path. A graph is said to be balanced if its in-degree (number of communication links arriving at the node) is equal to its out-degree (number of communication links leaving the node).

2.2 Saturation Function

Definition 1 Given a positive constant M, a function $\sigma : \mathbb{R} \to \mathbb{R}$ is said to be a linear saturation for M if it is continuous, nondecreasing function satisfying (Fig. 2)

1. $s\sigma(s) > 0$ for all $s \neq 0$;
2. $\sigma(s) = s$ when $| s | \leq M$;
3. $| \sigma(s) | \leq M$ for all $s \in \mathbb{R}$

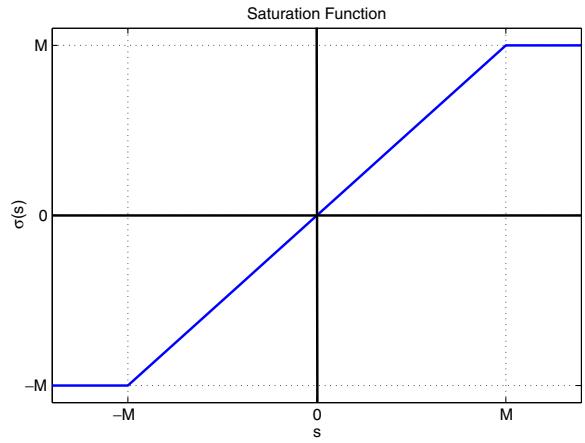

Fig. 2 Saturation function

2.3 Dynamic Model

Since the purpose of this work is to develop a miniquadrotor formation flight control, let us consider the dynamical model introduced in [13]:

$$\ddot{x} = -F_T \sin(\theta), \tag{1}$$

$$\ddot{y} = F_T \cos(\theta)\sin(\phi), \tag{2}$$

$$\ddot{z} = F_T \cos(\theta)\cos(\phi) - 1, \tag{3}$$

$$\ddot{\phi} = \tau_\phi, \tag{4}$$

$$\ddot{\theta} = \tau_\theta, \tag{5}$$

$$\ddot{\psi} = \tau_\psi, \tag{6}$$

where F_T is the thrust force vector in the body system, (x, y, z), (ϕ, θ, ψ) and $(\tau_\phi, \tau_\theta, \tau_\psi)$ represent the quadrotor position, orientation and torque control respectively.

Remark that, there are other ways to represent the orientation of rigid bodies, e.g. quaternion; however for the purpose of this work, Euler angles represent a simple and practical solution to be adopted.

3 Control Design

In this section, a nonlinear controller with a coordination control strategy is developed. First, it will be proved that, the proposed control scheme stabilizes the quadrotor in hover flight. It will then be proved that a coordination control algorithm

combined with the proposed nonlinear control stabilizes the quadrotor formation flight.

3.1 Vehicle Stabilization

In order to stabilize the altitude and the heading of the mini rotorcraft, the following control inputs are proposed

$$F_T \triangleq \frac{-a_1\dot{z} - a_2(z - z^d) + 1}{\cos(\phi)\cos(\theta)}, \tag{7}$$

$$\tau_\psi \triangleq -a_3\dot{\psi} - a_4(\psi - \psi^d), \tag{8}$$

where a_1, a_2, a_3 and a_4 are positive constant; z^d and ψ^d are the desired altitude and heading, respectively. Notice that, the control inputs (7) and (8) stabilize the altitude and heading in closed-loop system, such that

$$\lim_{t\to\infty} \left\| z - z^d \right\| \to 0,$$

$$\lim_{t\to\infty} \left\| \psi - \psi^d \right\| \to 0.$$

Consequently, introducing Eq. 7 into Eq. 2 the lateral dynamic model is represented by the following set of equations:

$$\ddot{y} = \tan\phi,$$

$$\ddot{\phi} = \tau_\phi.$$

Similarly, the longitudinal dynamic model is represented by

$$\ddot{x} = \frac{-\tan\theta}{\cos\phi}, \tag{9}$$

$$\ddot{\theta} = \tau_\theta. \tag{10}$$

It is assumed that, pitch and roll angle will be operated in a neighborhood of the origin, i.e., $|\phi| < \pi/10$. Moreover, the proposed control approach provides an upper bound for the attitude subsystem such that, $\tan\phi \approx \phi$. Then, the lateral dynamical system can be reduced to

$$\ddot{y} = \phi, \tag{11}$$

$$\ddot{\phi} = \tau_\phi. \tag{12}$$

Notice that, the previous system represents four integrators in cascade. In order to introduce the consensus algorithm let us consider the following system

$$\chi^{(4)} = u(\chi). \tag{13}$$

Theorem 1 *Consider the system in Eq. 13. Then, the following control law*

$$u(\chi) = -\sigma_4(\kappa_4) - \sigma_3(\kappa_3) - \sigma_2(\kappa_2) - \sigma_1(\kappa_1), \tag{14}$$

with

$$\kappa_1(\chi) = \kappa_2 - \chi - 2\dot{\chi} + \ddot{\chi}, \tag{15}$$

$$\kappa_2(\chi) = \kappa_3 + \ddot{\chi} - \dot{\chi}, \tag{16}$$

$$\kappa_3(\chi) = \kappa_4 + \ddot{\chi}, \tag{17}$$

$$\kappa_4(\chi) = \chi^{(3)}, \tag{18}$$

makes the closed loop system stable.

Proof To simplify the analysis, a recursive methodology is proposed. Let us assume that

$$\zeta_n = \sigma_n(\kappa_n) + \zeta_{n-1},$$

$$\zeta_1 = \sigma_1(\kappa_1),$$

and

$$\dot{\kappa}_n = u = -\zeta_n.$$

Define the following positive definite function

$$V_n = \frac{1}{2}\kappa_n^2.$$

Differentiating V with respect to time, the above yields,

$$\dot{V}_n = \kappa_n\dot{\kappa}_n = -\kappa_n\zeta_n,$$

$$= -\kappa_n\left(\sigma_n(\kappa_n) + \zeta_{n-1}\right).$$

Using Definition 1 and proposing $M_{n-1} < 0.5M_n$, it can be noted that, if $|\kappa_n| > 0.5M_n$, then, $\dot{V}_n < 0$. This means that, there exist a time T_n, such that, $|\kappa_n| \le 0.5M_n$ for $\forall t > T_n$, which implies that $|\kappa_n(\chi) + \zeta_{n-1}| \le 0.5M_n + M_{n-1} \le M_n$.

The base case of the recursion occurs when the V_1 function is analyzed and this case will be treated a little different. Propose

$$V_1 = \frac{1}{2}\kappa_1^2.$$

Differentiating the above with respect to time and using Eqs. 15–18, it is follows that

$$\dot{V}_1 = \kappa_1 \dot{\kappa}_1 = -\kappa_1 \sigma_1(\kappa_1).$$

Notice from the above that, $\dot{V}_1 < 0$, then, this implies that κ_1 and $\zeta_1 \to 0$. Observe that, $\forall\ i = 2, ..., n$, the following set of equations are obtained,

$$\dot{V}_2 = -\kappa_2(\sigma_2(\kappa_2) + \zeta_1), \tag{19}$$

$$\dot{V}_3 = -\kappa_3(\sigma_3(\kappa_3) + \zeta_2), \tag{20}$$

$$\dot{V}_4 = -\kappa_4(\sigma_4(\kappa_4) + \zeta_3), \tag{21}$$

with

$$\zeta_2 = \sigma_2(\kappa_2) + \zeta_1, \tag{22}$$

$$\zeta_3 = \sigma_3(\kappa_3) + \zeta_2, \tag{23}$$

$$\zeta_4 = \sigma_4(\kappa_4) + \zeta_3. \tag{24}$$

Note that, from Eq. 19, $\kappa_2 \to 0$, and from Eq. 22 implies that $\zeta_2 \to 0$. In the same way, from Eq. 20, $\kappa_3 \to 0$ and this implies from Eq. 23 that $\zeta_3 \to 0$. Similarly, from Eq. 21, $\kappa_4 \to 0$, and from Eq. 24, $\zeta_4 \to 0$. This implies that, from Eq. 18, $\chi^{(3)} \to 0$, which follows that, from Eq. 17, $\ddot{\chi} \to 0$, in addition, from Eq. 16, $\dot{\chi} \to 0$, and finally from Eq. 15, $\chi \to 0$. □

Therefore, the lateral control law can be stated like

$$\tau_\phi = -\sigma_4(\dot{\phi}) - \sigma_3(\dot{\phi} + \phi) - \sigma_2(\dot{\phi} + 2\phi + \dot{y}) - \sigma_1(\dot{\phi} + 3\phi + 3\dot{y} + y). \tag{25}$$

Notice from the previous control analysis that, $\dot{\phi}, \phi, \dot{y}$ and $y \to 0$. Then, from Eqs. 9 and 10, the system is reduced to four integrators in cascade. Hence, we can propose

$$\tau_\theta = -\sigma_4(\dot{\theta}) - \sigma_3(\dot{\theta} + \theta) - \sigma_2(\dot{\theta} + 2\theta - \dot{x}) - \sigma_1(\dot{\theta} + 3\theta - 3\dot{x} - x). \tag{26}$$

Remark 1 The bounded saturations control used in mini UAVs are classified as either nested or separated saturations. The difference between them is the convergence time, as described in [25], due the fact that the states converge from the saturated zone to the linear zone quickly in the case of separated saturations.

3.2 Consensus Agreement

One of the problems of working with multiple autonomous vehicles is the collision avoidance. A coordination strategy to ensure the formation and collision avoidance at the same time is here proposed. It should be noticed that a multi-agent approach ensures the flock centering as well as the collision avoidance among multi-agents. To develop this approach, we will start by analyzing the longitudinal kinematic model for the multi-quadrotor system which is given by

$$\dot{\mathrm{x}} = -\mathcal{L}\mathrm{x}, \tag{27}$$

where $\mathcal{L}$ is the Laplacian matrix of the information exchange graph having the following properties:

1. $\mathcal{L}$ has a single eigenvalue at 0, $\lambda_1(\mathcal{L}) = 0$ with right eigenvector $w_1^T = \begin{bmatrix} 1\ 1 \cdots 1 \end{bmatrix}$, *i.e.* $\mathcal{L}w_1 = 0$.
2. The remaining eigenvalues are all positive, i.e. $\lambda_i(\mathcal{L}) > 0$ and $\mathcal{L}w_i = \lambda_i w_i$ for $i = 2, ..., n$, and $w_i \in R^n$.

We assume that, the information exchange graph is balanced. Let us assume also that in the coordinating controller the gains multiplying the signals in between agents are all equal to 1. For the $i-th$ row of $\mathcal{L}$, the entries $l_{ij} = -1$ for $i \neq j$ correspond to the gains multiplying the signals from other agents coming to agent i. For the $i-th$ column of $\mathcal{L}$, the entries $l_{ji} = -1$ for $i \neq j$ correspond to the gains multiplying the signals going out of agent i towards the other agents. Then, the following property is also necessary

3. w_1, defined above, is also the left eigenvector of $\mathcal{L}$ corresponding to the eigenvalue 0, i.e. $w_1^T\mathcal{L} = 0$.

It is worth to mention that, dynamics (27) can also be written as

$$\dot{x}_i = \bar{u}_i, \qquad \forall i = 1, ..., n;$$

with multiple agent consensus achieved using the following forced consensus algorithm

$$\bar{u}_i = -\sum_{j\in\mathcal{N}_i}(x_i - x_j),$$

where $\mathcal{N}_i$ is the set of vehicles transmitting their information to the vehicle i.

Observe that, when using Eqs. 25 and 26 all the states goes to the origin. And since, the control objective is to force the consensus of a set of quad-rotor vehicles to a desired position and heading, we propose the following change of variables

$$x \triangleq \sum_{j\in\mathcal{N}_i}(x_j - x_i), \tag{28}$$

$$y \triangleq \sum_{j\in\mathcal{N}_i}(y_j - y_i), \tag{29}$$

$$z \triangleq \sum_{j\in\mathcal{N}_i}(z_j - z_i), \tag{30}$$

$$\psi \triangleq \sum_{j\in\mathcal{N}_i}(\psi_j - \psi_i), \tag{31}$$

where x_i, y_i, z_i, ψ_i, x_j, y_j, z_j and ψ_j represent the 3D position and heading of the i-th quad-rotor and the j-th quad-rotor to be coordinated.

Remark 2 On one hand a multiple mini rotorcraft consensus can be achieved by means of a single integrator consensus algorithm, then, Eqs. 28 and 29 provide a simple way to solve the coordination problem. On the other hand, we may think of the neighbors position of a mini rotorcraft as the position reference and thus the stability of every mini rotorcraft is guaranteed using the nonlinear control based on separated saturations.

From the previous control analysis, we have that $x \to 0$, $y \to 0$, $z \to z^d$ and $\psi \to \psi^d$, and from Eqs. 28 and 29, this implies that

$$\lim_{t\to\infty} \|x_j - x_i\| = 0, \tag{32}$$

$$\lim_{t\to\infty} \|y_j - y_i\| = 0. \tag{33}$$

From Eqs. 7, 8, 30 and 31, we have that

$$\lim_{t\to\infty} \|z_j - z_i\| = z^d, \tag{34}$$

$$\lim_{t\to\infty} \|\psi_j - \psi_i\| = \psi^d. \tag{35}$$

Therefore, the control laws τ_θ, τ_ϕ, τ_ψ and F_T for the longitudinal, lateral, heading and altitude subsystems of the ith-minirotorcraft becomes

$$\tau_{\theta_i} = -\sigma_4\left(\dot{\theta}_i\right) - \sigma_3\left(\dot{\theta}_i + \theta_i\right) - \sigma_2\left(\dot{\theta}_i + 2\theta_i - \dot{x}_i\right) - \sigma_1\left(\dot{\theta}_i + 3\theta_i - 3\dot{x}_i - \left(\sum_{j\in\mathcal{N}_i}\left(x_j - x_i\right)\right)\right), \tag{36}$$

$$\tau_{\phi_i} = -\sigma_4\left(\dot{\phi}_i\right) - \sigma_3\left(\dot{\phi}_i + \phi_i\right) - \sigma_2\left(\dot{\phi}_i + 2\phi_i + \dot{y}_i\right) - \sigma_1\left(\dot{\phi}_i + 3\phi_i + 3\dot{y}_i - \left(\sum_{j\in\mathcal{N}_i}\left(y_j - y_i\right)\right)\right), \tag{37}$$

$$F_T = \frac{-a_1\dot{z} - a_2\left(\sum_{j\in\mathcal{N}_i}\left(z_j - z_i\right) - z^d\right) + 1}{\cos(\phi)\cos(\theta)}, \tag{38}$$

$$\tau_\psi = -a_3\dot{\psi} - a_4\left(\sum_{j\in\mathcal{N}_i}\left(\psi_j - \psi_i\right) - \psi^d\right). \tag{39}$$

Note that Eqs. 36–39 enable us to stabilize the coordination for a group of n minirotorcraft. We also notice that in practice due to the fact that a coordination to a fixed position implies that every mini rotorcraft will converge to the same position in the 3D space producing the collision of all mini rotorcrafts. In order to solve this problem, a simple leader relative position control is developed in the next section.

3.3 Formation Control

In this section, we propose a leader-relative position consensus (UAV formation) for the multi quadrotor system, i.e. the quadrotor vehicles will converge to a position with respect to the leader of the group.

Let us define a relative position with respect to its neighbors as follows

$$x_i - x_j = x_i^d, \tag{40}$$

where x_i^d is a positive constant.

Using a relative position reference for the flight formation of multiple mini rotorcraft, Eqs. 36–39 are rewritten as

$$\tau_{\theta_i} = -\sigma_4\left(\dot{\theta}_i\right) - \sigma_3\left(\dot{\theta}_i + \theta_i\right) - \sigma_2\left(\dot{\theta}_i + 2\theta_i - \dot{x}_i\right) - \sigma_1\left(\dot{\theta}_i + 3\theta_i - 3\dot{x}_i - \left(\sum_{j\in\mathcal{N}_i}\left(x_j - x_i\right) - x_i^d\right)\right), \tag{41}$$

$$\tau_{\phi_i} = -\sigma_4\left(\dot{\phi}_i\right) - \sigma_3\left(\dot{\phi}_i + \phi_i\right) - \sigma_2\left(\dot{\phi}_i + 2\phi_i + \dot{y}_i\right) - \sigma_1\left(\dot{\phi}_i + 3\phi_i + 3\dot{y}_i - \left(\sum_{j\in\mathcal{N}_i}\left(y_j - y_i\right) - y_i^d\right)\right), \tag{42}$$

where x_i^d, y_i^d, z_i^d and ψ_i^d are the desired geometrical 3D position and heading reference with respect to the leader as shown in previous section. Thus, Eqs. 38, 39, 41 and 42 are such that, the geometric flight formation of the multiple mini rotorcraft system is guaranteed.

In order to exemplify the proposed approach, let us consider the case of three quadrotors with the following information flow topologies: cyclic and chain, see Fig. 3.

Definition 2 A chain topology of information exchange or cyclic information flow topology is one in which agent i and agent $(i+1)$ mutually exchange their informations as shown in Fig. 3a.

Definition 3 A cyclic topology of information exchange or cyclic information flow topology is one in which agent i receives information from agent $((i+1) \mod n)$ as shown in Fig. 3b.

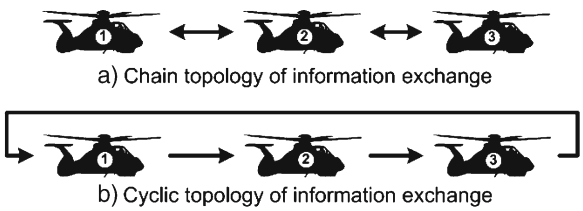

Fig. 3 Cyclic and chain topologies of information exchange

Triangular Formation A triangular formation around a circle of radius r for a team of three quadrotor vehicles is proposed, see Fig. 1. Assuming a cyclic information flow topology, the relative position is given by

$$x_1 - x_2 = r\cos(\pi/6), \tag{43}$$

$$x_3 - x_1 = -r\cos(\pi/6), \tag{44}$$

$$x_2 - x_3 = r\cos(\pi/2), \tag{45}$$

$$y_1 - y_2 = r\sin(\pi/6), \tag{46}$$

$$y_3 - y_1 = -r\sin(\pi/6), \tag{47}$$

$$y_2 - y_3 = 2r\sin(\pi/6). \tag{48}$$

Assuming a chain information exchange topology, the relative position is given by

$$x_1 - x_2 = \cos(\pi/6), \tag{49}$$

$$x_2 - x_3 = \cos(\pi/2), \tag{50}$$

$$y_1 - y_2 = \sin(\pi/6), \tag{51}$$

$$y_2 - y_3 = 2\sin(\pi/6). \tag{52}$$

Therefore, we can use either Eqs. 43–48 or Eqs. 49–52 as a relative position reference x_i^d and y_i^d with respect to each other. Note that the desired altitude for the platoon is set to a positive constant $z^d > 0$ and the desired heading can be set to a constant $\psi^d \in [-\pi, \pi]$.

Line Formation For a team of three quadrotor vehicles assuming chain information exchange topology, the relative position for a line formation over the y-axis is given by

$$x_i - x_j = 0, \tag{53}$$

$$y_i - y_j = d_{ij}, \tag{54}$$

where d_{ij} is a fixed distance between any two mini rotorcraft. Similarly, the relative position for a line formation over the x-axis is given by

$$x_i - x_j = d_{ij}, \tag{55}$$

$$y_i - y_j = 0. \tag{56}$$

Therefore, we can use either Eqs. 53 and 54 or Eqs. 55 and 56 as a relative position reference x_i^d

and y_i^d with respect to each other. Observe that, for a line formation along any axis, the relative position of an agent with respect to its neighbors is the same for any information exchange topology.

Remark 3 It is important to remark that the geometrical formations can be extended to the case of n agents or minirotorcrafts by defining the proper neighbor-relative position references or by using flocking methods as in [15–17].

3.4 X4 Trajectory Tracking Control

Now, we will consider the case of trajectory tracking of a multiple vehicle system. It is assumed that, the leader of the group is always vehicle 1. Then, Eq. 27 can be rewritten as

$$\dot{\mathbf{x}} = -\mathcal{L}\mathbf{x} + \mathbf{b}u_{1_x}, \tag{57}$$

where $\mathbf{b}^T = [1\ 0\ \ldots\ 0]$ and u_{1_x} is the input given to the leader. Define,

$$x_{CM} = \frac{1}{N}\sum_{i=1}^{N} x_i,$$

where N is the number of agents in the formation. Let x_{CM}^d be the desired value for x_{CM}. Thus, u_{1_x} can be stated as

$$u_{1_x} = Nk\,\sigma(x_{CM}^d - x_{CM}), \tag{58}$$

where $\sigma(\cdot)$ represents the saturation function and k is a positive gain. Note that, x_{CM} may not be directly measurable for the leader (vehicle 1). Notice that, for a cyclic topology of information exchange, the system is observable from the input and output of the leader. The state can therefore be observed from the input and output of vehicle 1. Introducing Eq. 58 into Eq. 57, it is follows that

$$\dot{x}_{CM} = k\,\sigma\left(x_{CM}^d - x_{CM}\right),$$
$$v_i^T\mathbf{x} = -\lambda_i(v_i^T\mathbf{x}) + v_i^T\mathbf{b}u_{1_x}, \qquad \forall\, i = 2, \ldots, N.$$

All the modes in the above equation are stable. When $u_{1_x} = 0$, these modes converge to zero which means that, $(x_i - x_j) \to 0$ for $i \neq j$. This property is obtained by using the coordinating control algorithm that leads the position dynamics to Eq. 57. These modes are uncontrollable when $v_i^T\mathbf{b} = 0$. In addition, there is a trade-off in the choice of gain k in Eq. 58. For smaller values of k, the speed of convergence of x_{CM} is slower, but the transient in the errors $(x_i - x_j)$ for $i \neq j$, will be smaller, see [26].

Then, the trajectory tracking control for the leader of the group is given by

$$\begin{aligned}\tau_{\theta_1} = {} & -\sigma_4\left(\dot{\theta}_i\right) - \sigma_3\left(\dot{\theta}_i + \theta_i\right) - \sigma_2\left(\dot{\theta}_i + 2\theta_i - \dot{x}_i\right) \\ & -\sigma_1\left(\dot{\theta}_i + 3\theta_i - 3\dot{x}_i \right. \\ & \left. -\left(\sum_{j\in\mathcal{N}_i}\left(x_j - x_i\right) - x_i^d - u_{1_x}\right)\right), \end{aligned} \tag{59}$$

$$\begin{aligned}\tau_{\phi_1} = {} & -\sigma_4\left(\dot{\phi}_i\right) - \sigma_3\left(\dot{\phi}_i + \phi_i\right) - \sigma_2\left(\dot{\phi}_i + 2\phi_i + \dot{y}_i\right) \\ & -\sigma_1\left(\dot{\phi}_i + 3\phi_i + 3\dot{y}_i \right. \\ & \left. -\left(\sum_{j\in\mathcal{N}_i}\left(y_j - y_i\right) - y_i^d - u_{1_y}\right)\right). \end{aligned} \tag{60}$$

Remark 4 Once the geometric formation has been achieved, the proposed control Eqs. 59 and 60 guarantees the collision avoidance among quadrotors.

4 Results

4.1 Simulation results

To illustrate the proposed methodology, this section presents the simulation results concerning the multiple miniature quadrotor formation control. We consider three miniature quadrotors evolving in the 3D space. Extensive simulations were run on a platoon of three rotorcrafts considering the 6-DOF nonlinear dynamical model. Cyclic and chain topologies of information exchange were considered.

In order to reproduce a realistic scenario, take-off initial conditions have been considered in simulations. Then, the initial euler angles, angular

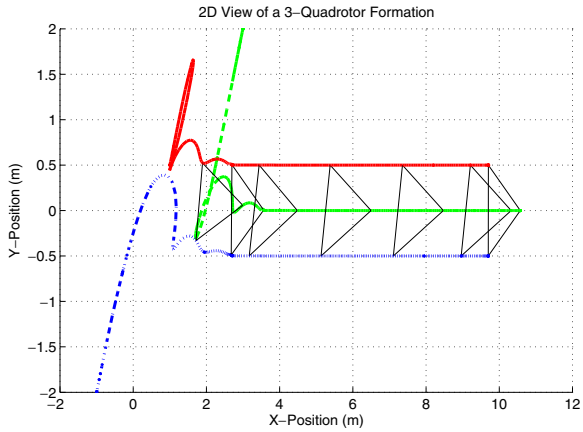

Fig. 4 Flight formation performance over a cyclic topology of information exchange (2D view)

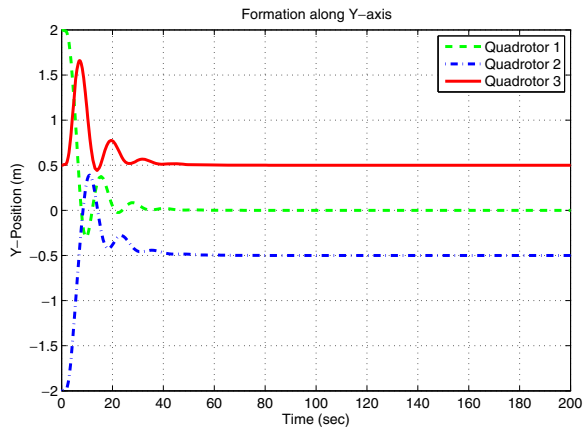

Fig. 6 Formation over Y-axis

velocities and initial velocities are all zero. The initial conditions for inertial position are:

$$[x_1, y_1, z_1] = [3, 2, 0]\text{m}, \tag{61}$$

$$[x_2, y_2, z_2] = [1, 0.5, 0]\text{m}, \tag{62}$$

$$[x_3, y_3, z_3] = [-1, -2, 0]\text{m}. \tag{63}$$

The simulation results show that the proposed nonlinear control strategy can be used to achieve a geometric formation as well as formation flying of multiple mini rotorcrafts. Thus, using control inputs 38–42 on the mini rotorcraft acting as followers and Eqs. 38, 39, 59 and 60 on the mini rotorcraft acting as leader, on the 6-DOF nonlinear dynamical model in simulation, we get the results shown in Fig. 4.

In this figure it is clear that the quadrotors achieve consensus and formation while converging to the given reference (or navigation point) for the center of mass $(3, 0)$m. After 60 s, the reference (navigation point) for the center of mass is changed to the 2D-coordinate $(10, 0)$m. During the formation flying process we can observe a slight misalignment of the formation which we attribute to a delay on the propagation of the new reference given only to the leader.

Figures 5 and 6 show formation over time for the longitudinal and lateral subsystems respectively.

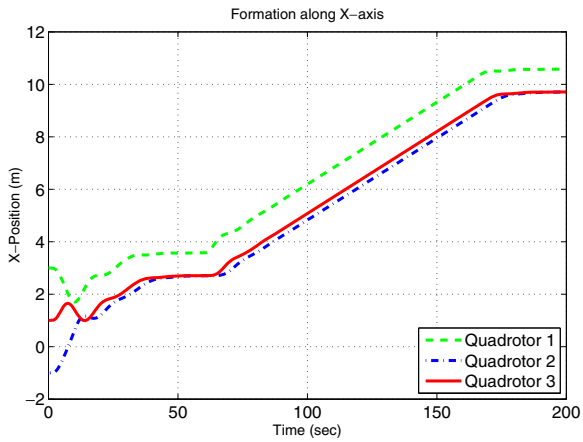

Fig. 5 Formation over X-axis

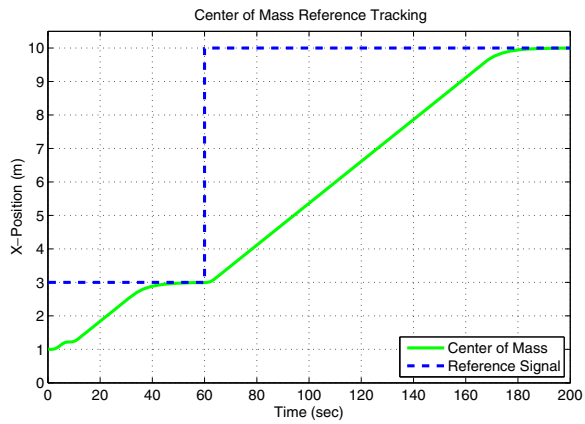

Fig. 7 Center of mass tracking

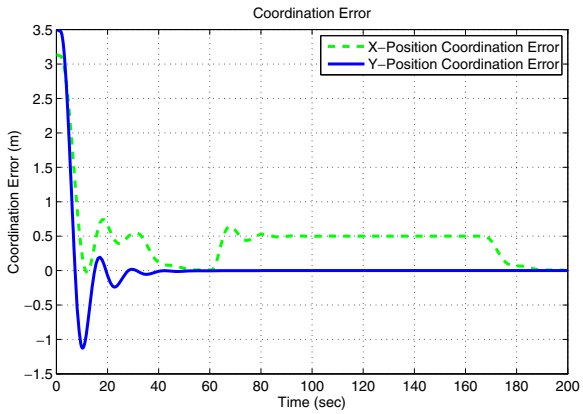

Fig. 8 Coordination error on lateral and longitudinal subsystems

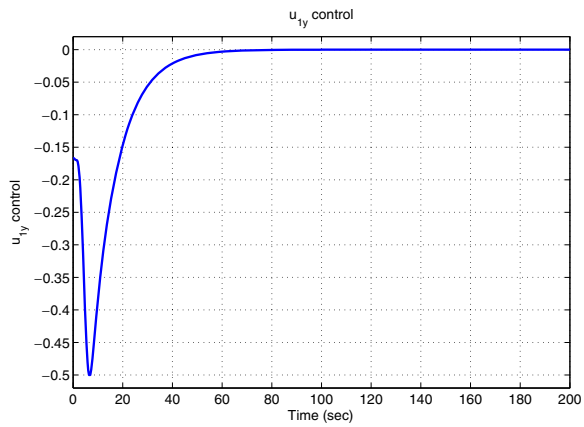

Fig. 10 u_{1_y} control. Saturation level 0.5

The tracking of the center of mass is shown in Fig. 7. We note that due to the fact that k is small ($k = 1.5$), the speed of convergence of the center of mass to the reference is slow but the transient in the errors $(x_i - x_j)$ and $(y_i - y_j)$, for $i \neq j$, are small.

Figure 8 shows the coordination error in the lateral and longitudinal subsystems. From this figure it is possible to confirm that the individual transient in errors $(x_i - x_j)$ and $(y_i - y_j)$ are small.

Figures 9, 10, 11 and 12 show the control inputs u_{1_x}, u_{1_y}, τ_x and τ_y. Note that the saturation levels used for longitudinal and lateral subsystems are 0.75 and 0.5, respectively.

4.2 Experimental Results

In this section, some experimental results on coordination are described. We validate some of the results presented in this section using two quadrotors provided of a IEEE 802.15.4 communication system. The control algorithm has been implemented on a microcontroller Rabbit RCM3400. Roll, pitch and yaw angles and angular rates are obtained using accelerometers, gyros and a compass. The experimental prototype design considers adding GPS functionality in future experiments. Actual GPS technologies provide between 5 and 10 m accuracy on the 3D position estimation.

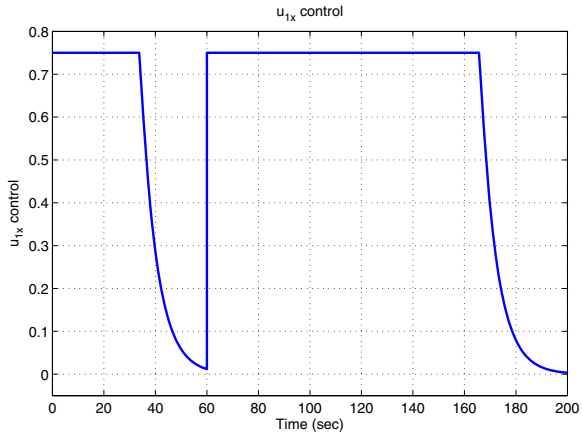

Fig. 9 u_{1_x} control. Saturation level 0.75

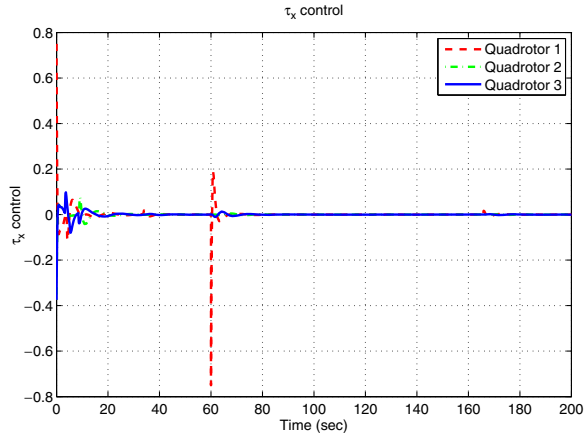

Fig. 11 τ_x control. Saturation level 0.75

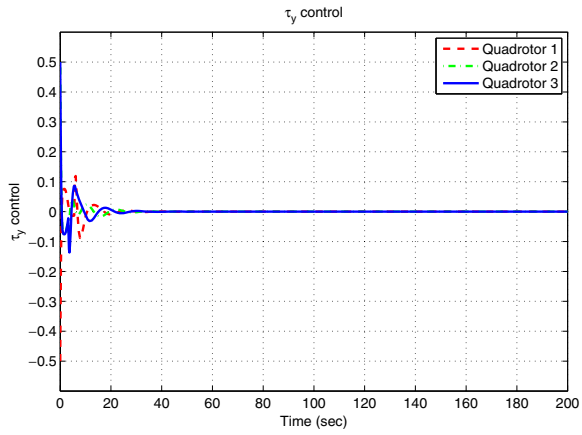

Fig. 12 τ_y control. Saturation level 0.5

As shown in previous sections, the proposed control algorithm stabilizes the formation flying of a small platoon of quadrotors. For safety reasons, the distributed algorithm has been implemented on the yaw subsystem only due to the fact that a failure either on the onboard control or communication systems will not produce a crashing of the experimental platforms. We remark that any failure on roll and pitch subsystems are critical and the immediate consequence is an experimental platform crash.

Figure 13 shows the performance of the coordination control over the yaw subsystem using control law Eq. 39. During the experiment, the reference for the yaw angle has been provided to the quadrotor leader using a R/C radio. The experimental results in Fig. 13 show that the quadrotor-follower was capable of tracking the heading of the leader. These experiments were run for about 100 s.

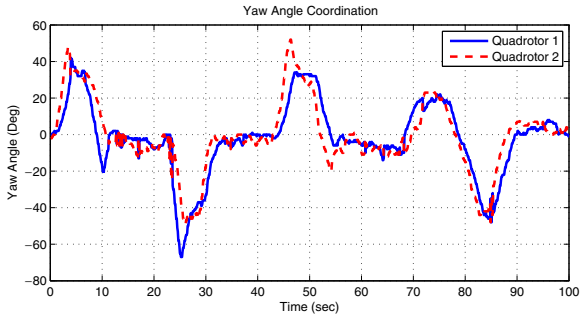

Fig. 13 Yaw coordination using control law Eq. 39

5 Conclusions and Future Work

A nonlinear dynamical model of the mini rotorcraft has been presented using the Newton-Euler formulation. Nonlinear control bounded inputs and a single integrator consensus control for flight formation of mini rotorcraft was developed. The x-position and the y-position of each mini rotorcraft were considered as dynamical agents with full information access. Trajectory tracking for the group of mini rotorcraft was achieved by using the virtual center of mass of the agents formation. Extensive simulations were run in order to show the performance of the developed control scheme. Heading coordination control approach has been implemented on two quadrotors using a IEEE 802.15.4 wireless dedicated network. Future work in this area includes extending the experimental tests to the case of formation keeping and formation flying using GPS modules on real-time embedded control systems.

References

1. Chen, X., Serrani, A.: ISS-based robust leader/follower trailing control. In: LNCIS 336 Group Coordination and Cooperative Control. Springer, Germany (2006)
2. Guerrero, J.A., Fantoni, I., Salazar, S., Lozano, R.: Flight formation of multiple mini rotorcraft via coordination control. In: IEEE International Conference on Robotics and Automation, Anchorage, Alaska (2010)
3. Guilietti, F., Pollini, L., Innocenti, M.: Autonomous formation flight. IEEE Control Syst. Mag. **20**(6), 34–44 (2000)
4. Leonard, N.E., Fiorelli, E.: Virtual leaders, artificial potentials and coordinated control of groups. In: Proceedings of the 40th IEEE Conf. on Decision and Control (2001)
5. Beard, R.W., Lawton, J., Hadaegh, F.Y.: A Coordination Architecture for Spacecraft Formation Control. IEEE Trans. Control Syst. Technol. **9**(6), 777–790 (2001)
6. Arrichiello, F., Chiaverini, S., Fossen, T.I.: Formation control of marine vessels using the null-space-based behavioral control. InL LNCIS 336 Group Coordination and Cooperative Control. Springer, Germany (2006)
7. Balch, T., Arkin, R.C.: Behavior-based formation control for multirobot teams. IEEE Trans. Robot. Autom. **14**(6), 926–939 (1998)
8. Bouabdallah, S., Noth, A., Siegwart, R.: PID vs LQ control techniques applied to an indoor micro quadrotor. In: Proc. of the IEEE/RSJ Int. Conf. Intelligent Robots and Systems, pp. 2451–2456 (2004)
9. Lara, D., Sanchez, A., Lozano, R., Castillo, P.: Real time embedded control system for VTOL aircrafts:

application to stabilize a quad-rotor helicopter. In: Proceedings of the IEEE Conference on Control Applications (2006)
10. Erginer, B., Altug, E.: Modeling and PD control of a quadrotor VTOL vehicle. In: IEEE Intelligent Vehicles Symposium, pp. 894–899 (2007)
11. La Civita, M., Papageorgiou, G., Messner, W.C., Kanade, T.: Design and flight testing of a gain-scheduled H_∞ loop shaping controller for wide-envelope flight of a robotic helicopter. In: Proc. of the 2003 American Control Conference, pp. 4195–4200 (2003)
12. Isidori, A., Marconi, L., Serrani, A.: Robust nonlinear motion control of a helicopter. IEEE Trans. Automat. Contr. **48**(3), 413–426 (2003)
13. Lozano, R.: Objets volants miniatures: modelisation et commande embarquee. Hermes–Lavoisier (2007)
14. Castillo, P., Lozano, R., Dzul, A.: Stabilization of a mini-rotorcraft having four rotors. IEEE Control Syst. Mag. **25**(6), 45–55 (2005)
15. Tanner, H.G., Jadbabaie, A., Pappas, G.J.: Stable flocking of mobile agents, part I: fixed topology. In: Proceedings of the 42nd IEEE Conference on Decision and Control, Maui (2003)
16. Tanner, H.G., Jadbabaie, A., Pappas, G.J.: Stable flocking of mobile agents, part II: dynamic topology. In: Proceedings of the 42nd IEEE Conference on Decision and Control, Maui (2003)
17. Olfati-Saber, R.: Flocking for multi-agent dynamic systems: algorithms and theory. IEEE Trans. Automat. Contr. **51**(3), 401–420 (2006)
18. Ren, W.: Consensus seeking in multi-vehicle systems with a time varying reference state. In: Proceedings of the 2007 IEEE American Control Conference, NY (2007)
19. Lee, D.J., Li, P.Y.: Formation and maneuver control of multiple spacecraft. In: Proceedings of the IEEE American Control Conference, Denver (2003)
20. Lee, D.J., Spong, M.W.: Flocking of multiple inertial agents on balanced graph. In: Proceedings of the IEEE American Control Conference (2006)
21. Hokayem, P., Stipanovic, D., Spong, M.W.: Reliable control of multi-agent formations. In: Proceedings of the IEEE American Control Conference, New York (2007)
22. Michael, N., Fink, J., Kumar, V.: Cooperative manipulation and transportation with aerial robots. In: Proc. of Robotics: Science and Systems, Seattle, WA (2009)
23. Oung, R., Bourgault, F., Donovan, M., D'Andrea, R.: The distributed flight array. In: IEEE International Conference on Robotics and Automation, Anchorage, Alaska (2010)
24. Godsil, C., Royle, G.: Algebraic graph theory. Springer (2001)
25. Sussmann, H.J., Sontag, E.D., Yang, Y.: A general result on the stabilization of linear systems using bounded controls. IEEE Trans. Automat. Contr. **39**(12), 2411–2425 (1994)
26. Lozano, R., Spong, M.W., Guerrero, J.A., Chopra, N.: Controllability and observability of leader based multi-agent systems. In: IEEE Conference on Decision and Control, Cancun, Mexico (2008)